Journal of Fluids and Structures (2000) **14,** 1173–1193
doi:10.1006/jfls.2000.0319, available online at http://www.idealibrary.com on IDEAL®

CHARACTERIZATION OF THE BEHAVIOUR OF A SIMPLE AEROSERVOELASTIC SYSTEM WITH CONTROL NONLINEARITIES

G. Dimitriadis and J. E. Cooper

Manchester School of Engineering, University of Manchester, Oxford Road Manchester M13 9PL, United Kingdom

(Received 12 October 1999, and in final form 10 July 2000)

The characterization of the behaviour of nonlinear aeroelastic systems has become a very important research topic in the Aerospace Industry. However, most work carried to-date has concentrated upon systems containing structural or aerodynamic nonlinearities. The purpose of this paper is to study the stability of a simple aeroservoelastic system with nonlinearities in the control system and power control unit. The work considers both structural and control law nonlinearities and assesses the stability of the system response using bifurcation diagrams. It is shown that simple feedback systems designed to increase the stability of the linearized system also stabilize the nonlinear system, although their effects can be less pronounced. Additionally, a nonlinear control law designed to limit the control surface pitch response was found to increase the flutter speed considerably by forcing the system to undergo limit cycle oscillations instead of fluttering. Finally, friction was found to affect the damping of the system but not its stability, as long as the amplitude of the frictional force is low enough not to cause stoppages in the motion.

1. INTRODUCTION

Over the past two decades, there has been a pronounced increase in research concerning nonlinear aeroelasticity. It has been known for quite some time that aircraft contain a number of nonlinearities which can significantly affect the dynamic behaviour. These nonlinearities give rise to phenomena such as limit cycle oscillations (LCOs) that cannot occur if the system is linear. Consequently, it is impossible to model and predict such behaviour using a linear analysis. The influence of nonlinearities is getting greater with each new generation of aircraft; therefore, the aerospace industry is starting to address the need for improved nonlinear modelling and predictive capability. The whole area of prediction and characterization of LCOs due to aerodynamic, structural and control nonlinearities has been defined as being an area of critical research interest (Cooper & Noll 1995).†

Some early work on nonlinear aeroelasticity, e.g. by Woolston *et al.* (1955) showed that limited amplitude oscillations are nonlinear phenomena, and Breitbach (1978) identified a number of sources of nonlinearity in aircraft. Since then, several investigations of nonlinear aeroelastic behaviour have been conducted, most of which concentrated on structural and, in particular, aerodynamic nonlinearities. In this latter area, most work has concentrated upon the development of unsteady CFD solutions (AGARD 1998) primarily in the transonic region. Some recent notable exceptions are the experimental work reported

† Throughout this paper, the word *flutter* is used to denote an unstable divergent oscillation, whereas *limit cycle* oscillation is used to denote an oscillation of bounded amplitude.

0889–9746/00/111173 + 21 $35.00/0

in Holden *et al.* (1995) and Conner *et al.* (1997) as well as various numerical studies on structural nonlinearities, such as Kim & Lee (1996) and Price *et al.* (1995). There is a relative dearth of work in the field of Aeroservoelasticity, with the exception of such works as Zimmermann (1991) and Noll (1993).

The increasing power of modern computers allowed the use of increasingly computationally intensive mathematical tools for the characterization of nonlinear behaviour, such as bifurcation plots (Lee & Kim 1995) and parameter-space sections (Price *et al.* 1994). LCOs have been observed and explained in terms of Hopf bifurcations (Price *et al.* 1995), and the possibility of LCO control and suppression has also been investigated (Mastroddi & Morino 1996; Dimitriadis & Cooper 1999; Frampton & Clark 1999). However, the main subject of all this research has been structural nonlinearities and, to a lesser extent, aerodynamic nonlinearities (Morton & Beran 1999). Little research has been conducted into the effects of nonlinearities in the control system even though, with the advent of Active Control Technology (ACT), control systems are becoming increasingly nonlinear. The performance of nonlinear aeroservoelastic systems throughout the desired flight envelope as well as their interaction with nondesigned nonlinearities, such as backlash in the linkage elements of the control system, has not been thoroughly investigated. Most work on aeroservoelastic systems has consisted generally of case studies, such as Becker & Vaccaro (1995).

Frampton & Clark (1999) applied linear active control to a typical section airfoil with nonlinearity in the flap restoring spring. However, they concentrated on only one type of nonlinearity, namely freeplay. In this paper, the aeroservoelastic behaviour of a number of simple simulated systems with various nonlinearities is investigated and characterized. The purpose of the work is to give an overview of possible nonlinear behaviour that may occur as a result of the interaction of simple linear and nonlinear control systems with structural nonlinearities. The following nonlinearities are considered: (i) bilinear stiffness (zero-memory transducer nonlinearity); (ii) freeplay stiffness (zero-memory transducer nonlinearity); (iii) backlash (transducer nonlinearity with memory); (iv) friction (zero-memory transducer nonlinearity); (v) pitch limiting control system (control nonlinearity with memory).

2. SIMULATED AEROSERVOELASTIC SYSTEM

The basis of all the systems investigated in this work is an extension of the Hancock aeroelastic model (Hancock *et al.* 1985). The basic Hancock model is a rigid wing with two springs at the wing root, giving the system two degrees of freedom, heave and pitch. The aerodynamics is modelled using quasi-steady strip theory with approximate unsteady aerodynamic derivatives. The model used here also includes a control surface (Dimitriadis & Cooper 1999), i.e. it incorporates an additional degree of freedom. The control surface is driven by a power control unit (PCU) or power actuator. The PCU was modelled along the lines suggested in Wright (1975) to provide both stiffness and structural damping. The basic simulated system, which is shown in Figure 1, was modified by the addition of four typical structural nonlinearities (bilinear spring, freeplay, backlash and friction) along with three controllers (feedback, delayed feedback and pitch limits).

3. STRUCTURAL NONLINEARITIES

The PCU contains a pressure feedback spring, as shown in Figure 2. The modelling of the stiffness nonlinearities in the PCU followed the analysis in Maharaj *et al.* (1991)

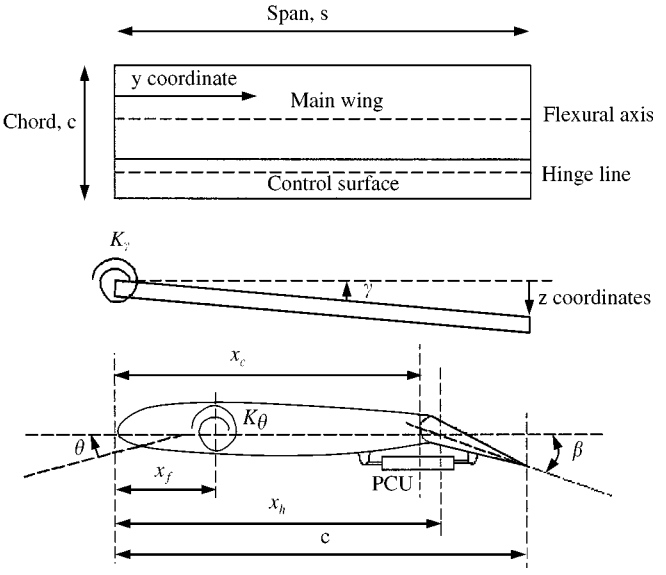

Figure 1. Basic Hancock model with control surface and PCU.

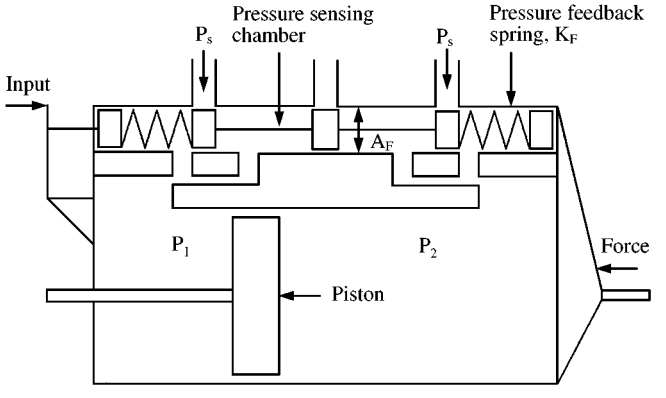

Figure 2. Power control unit.

3.1. Bilinear PCU Spring

The first system examined in this paper has a bilinear pressure feedback spring. Bilinear stiffness is a piecewise linear function shown in Figure 3. The stiffness, K_1, in the inner region (delimited by $\pm\delta$ in Figure 3) is lower than the stiffness in the outer region, K_2.

This is not a straightforward case of bilinear stiffness in the control surface since, because the bilinear spring is in the PCU, it affects the control surface velocity as well as displacement. The PCU equation is

$$\frac{VK_F}{4N}\dot{P}_J + K_V A_F\sqrt{P_s/2}P_J = dK_F A_P\dot{\beta} + \mu dK_F K_V\sqrt{P_s/2}(\beta - \beta_i), \tag{1}$$

where V is the volume of the PCU, N is the bulk modulus of oil, P_J is the difference of pressures in the two PCU compartments P_1 and P_2 (see Figure 2), K_V is a valve flow constant, A_F is the effective area of the pressure sensing chamber, P_s is the supply pressure,

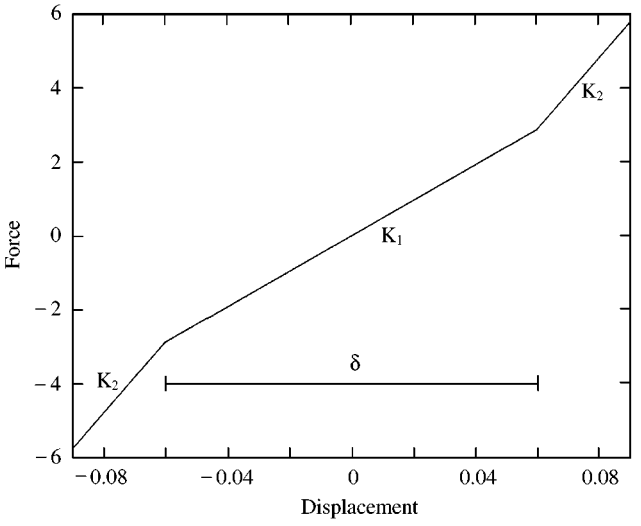

Figure 3. Bilinear stiffness versus displacement.

K_F is the stiffness of the pressure feedback spring, μ is the lever arm ratio, d is the distance between the PCU axis and the wing chord, β is the control surface deflection and β_i is the demand angle. It can be seen that K_F multiplies both the $\dot{\beta}$ and β terms. Hence, a nonlinear pressure feedback spring affects both control surface velocity and displacement.

3.2. Freeplay in PCU Spring

For this system, the pressure feedback spring contains freeplay. Freeplay stiffness is also a piecewise linear function, depicted in Figure 4. In this case, the stiffness in the inner region is zero. Again, the freeplay affects both control surface velocity and displacement.

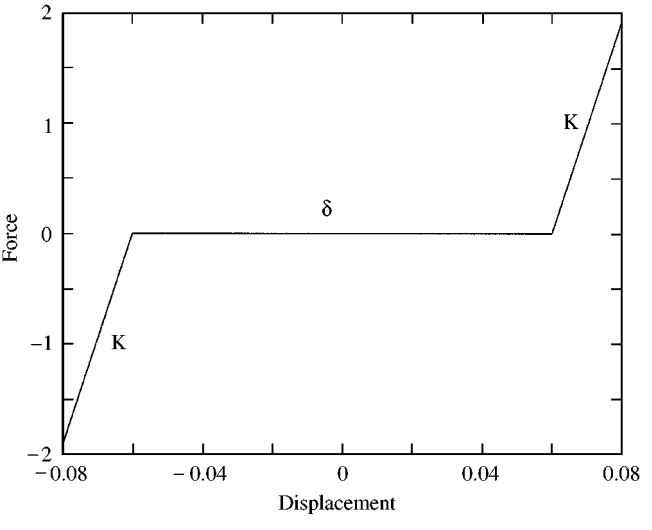

Figure 4. Freeplay stiffness versus displacement.

3.3. Backlash in PCU Spring

Backlash is a piecewise linear hysteretic nonlinearity. Figure 5 shows the variation of the force in the PCU with control surface deflection during a limit cycle oscillation (LCO), in the presence of backlash in the pressure feedback spring. Whenever the control surface pitch changes direction, the force in the PCU jumps from one of the sloped lines to the other. The horizontal distance between the two branches is called the backlash distance. Such behaviour can be observed for example in the bearings of all-movable control surfaces of military aircraft (Luber 1997). As with bilinear stiffness and freeplay, backlash affects both the velocity and displacement of the control surface of the system investigated here.

3.4. Friction in PCU

This case models friction between the piston seals and the chamber. The friction depends on the piston velocity, hence the force, F, in the piston is given by

$$F = A_p P_J + F_R \operatorname{sgn}(\dot{\beta}), \tag{2}$$

where F_R is the magnitude of the friction force. In all the simulations carried out for this project, it was assumed that F_R was low enough to allow movement of the piston without stoppages.

4. CONTROLLERS

4.1. Linear Feedback

A velocity and displacement feedback loop was added to the linear system, in order to increase the flutter speed. The velocity feedback increased the damping, while the displacement feedback increased the stiffness of the system. The demand angle, β_i, in equation (1) was written as

$$\beta_i = [c_1 \quad c_2 \quad c_3] \begin{Bmatrix} \dot{\gamma} \\ \dot{\theta} \\ \dot{\beta} \end{Bmatrix} + [k_1 \quad k_2 \quad k_3] \begin{Bmatrix} \gamma \\ \theta \\ \beta \end{Bmatrix}, \tag{3}$$

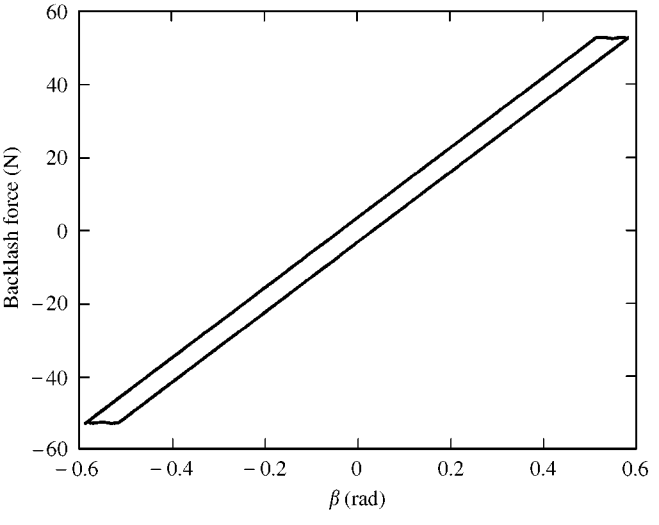

Figure 5. Backlash stiffness versus displacement.

TABLE 1
Open- and closed-loop dampings and natural frequencies of linear system at $V = 40$ m/s.

Open loop		Closed Loops	
Damping	Frequency (Hz)	Damping	Frequency (Hz)
0·0679	8·7682	0·0630	8·3956
0·0082	14·2815	0·0141	15·6221
0·0408	37·4495	0·1183	58·3950

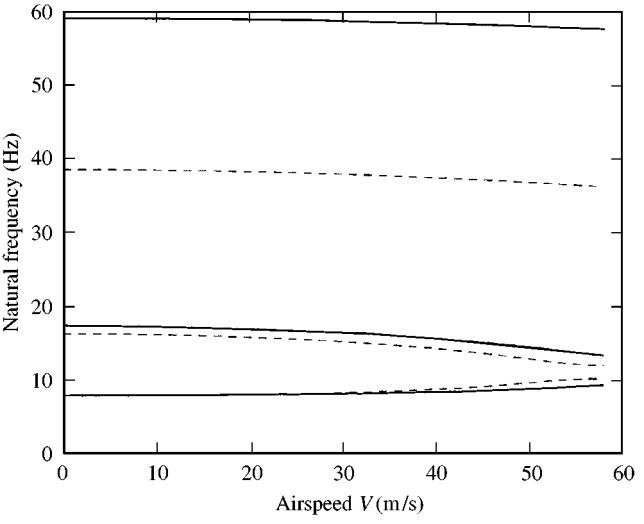

Figure 6. Open- and closed-loop natural frequencies of linear system: – – –, open loop; ——, closed loop.

where $c_1 \ldots c_3$ are the velocity feedback gains, $k_1 \ldots k_3$ are the displacement feedback gains and γ, θ and β are the degrees of freedom, as shown in Figure 1. Hence, the controller was designed to measure the degrees of freedom and to use them in order to synthesize the control signal.

In experimental implementations of active control for aeroelastic systems, such as Vipperman *et al.* (1998), the system is identified at a number of subcritical flight conditions and controllers are designed for each of these conditions. However, since in the present work the system is mathematical and fully defined in terms of dynamic pressure, a controller was designed which could be effective throughout the flight envelope. The feedback gains were chosen so as to (i) increase the flutter velocity by 20%, (ii) ensure that the control signal, β_i, never exceeds $\pm 15^\circ$, (iii) ensure that the control rate, $\dot{\beta}_i$, never exceeds 50°/s, (iv) the eigenvalues of the system remain complex, i.e. divergence does not occur.

The 20% target was chosen to comply with results presented in papers on flutter suppression such as Mukhopadhyay (1995). The changes in the natural frequencies at a speed of 40 m/s are tabulated in Table 1. Figures 6 and 7 show the open- and closed-loop natural frequencies and dampings, respectively, for a range of airspeeds. The figures show that the natural frequencies which combine to cause flutter are more separated in the closed-loop system than in the open-loop system. Additionally, the damping of the critical mode is higher in the closed-loop system. The consequent increase in flutter speed is 19·3%.

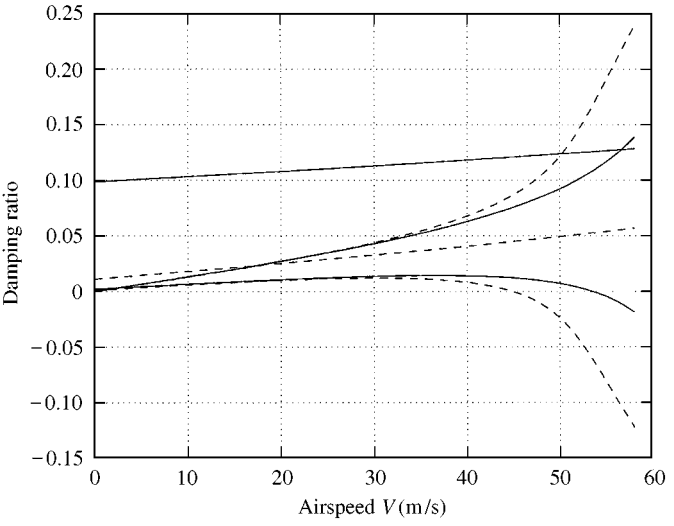

Figure 7. Open- and closed-loop damping ratios of linear system: – – –, open loop; ——, closed loop.

4.2. Delayed Feedback

To simulate the fact that real control systems do not act instantaneously, the feedback signal was delayed. It was found that a delay time equal to Δt (the integration time step, set to 0·001 s) decreased the effectiveness of the control system by decreasing the improvement in flutter speed to 16%. If the delay was increased to $2\Delta t$, then the system became unstable throughout the flight envelope. Noninteger multiples of the integration time step were also tested. In order to delay the feedback by a noninteger multiple of the time step, interpolation had to be used, resulting in much longer simulation times. It was found that the system remained stable up to a delay value of $1{\cdot}6\Delta t$. However, it was decided to stick to a delay value equal to Δt since this amount of delay was enough to demonstrate the decrease in the efficiency of the control system while allowing for shorter simulation times.

The delayed feedback control system was also used in conjunction with the freeplay, bilinear, backlash and friction nonlinearities mentioned above.

4.3. Control Surface Pitch Limit

An active control system was devised to limit the control surface pitch. Initially, it was assumed that the control system knows at all times the exact value of the control surface pitch. The pitch, β, at time t is used in conjunction with the value of the pitch at time $t - \Delta t$ to predict $\beta(t + \delta t)$ using linear curve-fitting, i.e.

$$\beta(t + \Delta t) = 2\beta(t) - \beta(t - \Delta t). \tag{4}$$

If $\beta(t + \Delta t)$ exceeds a given limit, β_{lim}, then the control system feeds back $-a\beta$ through the actuator, where a is a constant. Since a real control system would not be able to instantaneously complete all the calculations, acquire the current value of β and feed it to the actuator, the feedback in the simulated system is delayed by Δt. The feedback signal produced by this control scheme is plotted in Figure 8 against control surface pitch. The dashed lines show the pitch limits ($\pm$ 10° in this case). The feedback signal is zero at low values of β and equal to $-a\beta$ when β is near the limit.

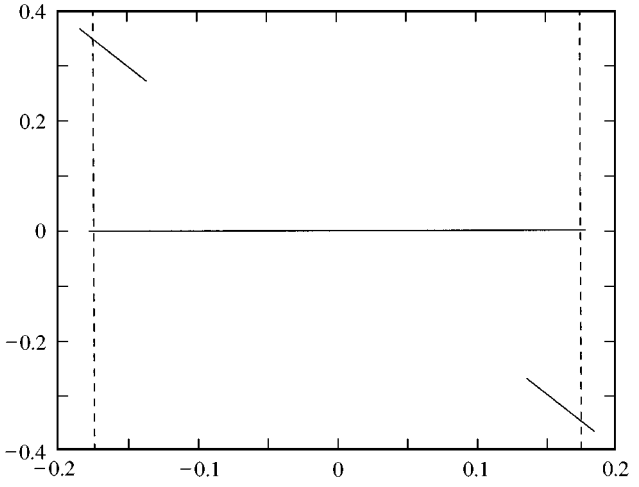

Figure 8. Nonlinear function of control surface pitch limiting control scheme: ——, feedback signal; – – –, $\pm 10^{\circ}$ pitch limit.

5. LIMIT CYCLE OSCILLATIONS AND BIFURCATION DIAGRAMS

For a single-degree-of-freedom system, a LCO is a limited amplitude oscillation occurring around a line singularity (a set of point singularities, in the same way that a line is a set of points) in the phase-plane called a limit cycle. Such a limit cycle can be seen in Figure 9 where a typical velocity ($\dot{\beta}$) against displacement (β) plot is shown. The resulting curve is the limit cycle. Limit cycles are singularities since they can either attract the phase trajectories (stable limit cycle) or repel them (unstable limit cycle) (Dimitriadis & Cooper 1999). In the case of Figure 9, where a stable limit cycle is shown, the system response will always wind onto the limit cycle both from the inside and from the outside. In turn, this signifies that the limit cycle cannot be crossed. A limit cycle can be classed as period-1, period-2, etc., depending on its complexity. Figure 9 shows a limit cycle with only one loop, i.e. period-1. A period-3 limit cycle, with three loops, can be seen in Figure 10.

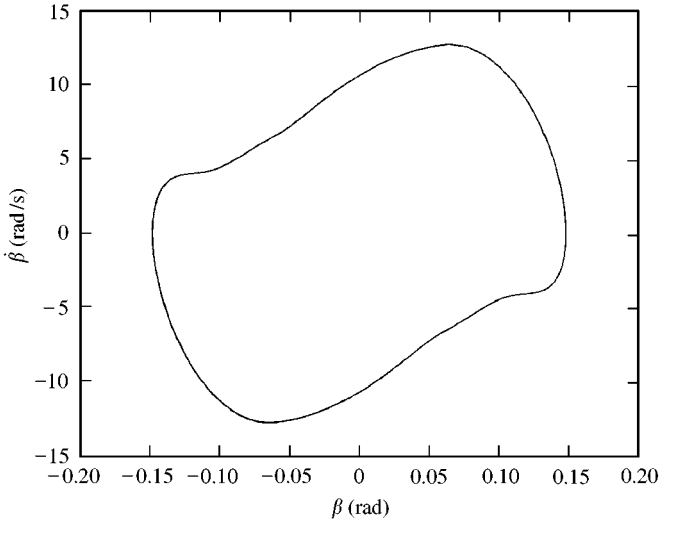

Figure 9. Phase-space diagram of a period-1 limit cycle for bilinear system with $V = 50$ m/s.

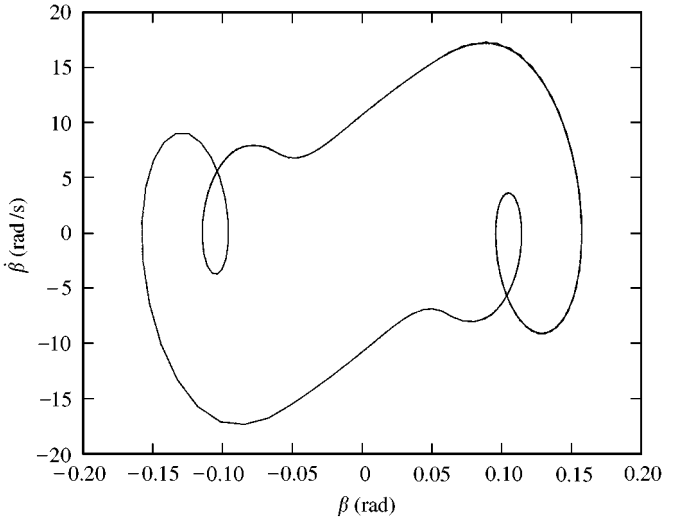

Figure 10. Phase-space diagram of a period-3 limit cycle for freeplay system with delayed feedback, $V = 50$ m/s.

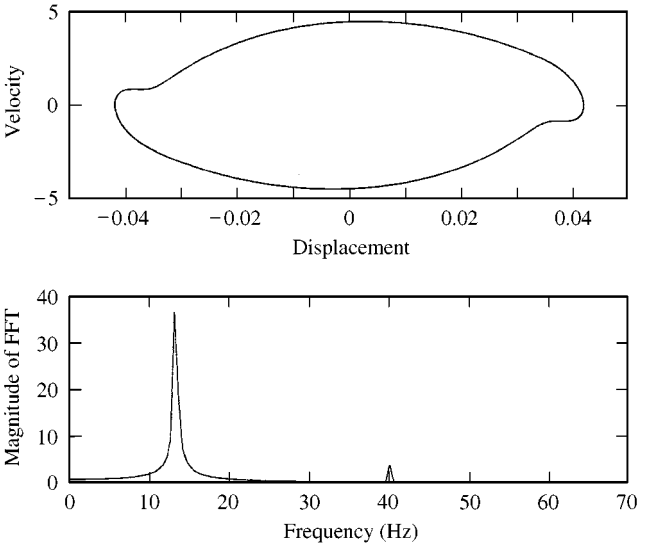

Figure 11. Fourier transform of a period-1 limit cycle.

For a multiple-degree-of-freedom system, a limit cycle is a multi-dimensional singularity, its dimensions being equal to the number of states in the system. However, limit cycles can still be visualized using phase-plane plots of the type shown in Figures 9 and 10, provided the velocity and displacement for the same degree-of-freedom (or mode) is plotted. The frequency content of a limit cycle can be obtained in the classical manner by taking the Fourier transform of the response. Figure 11 shows the Fourier transform of a period-1 limit cycle. Three frequency components exist at 13, 40 and 67 Hz. In general, the higher the period of a limit cycle, the more significant frequency components can be distinguished in the Fourier transform. Figure 12 shows the Fourier transform

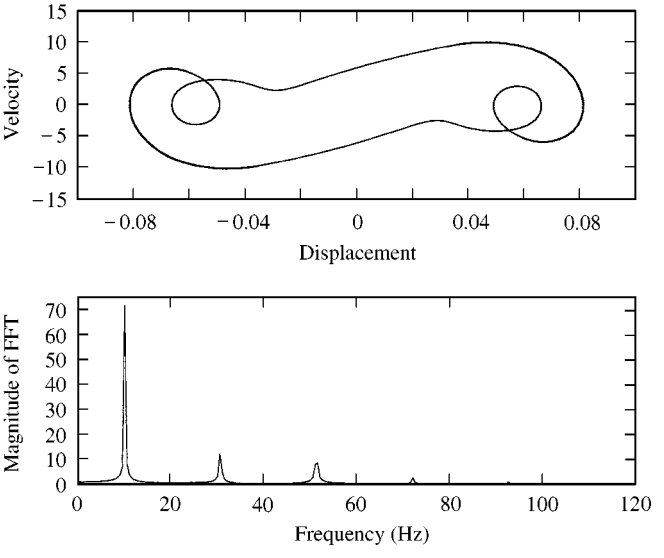

Figure 12. Fourier transform of a period-3 limit cycle.

of a period-3 limit cycle which contains five significant frequency components at 10, 31, 51, 72 and 93 Hz.

In the case of aeroelastic systems, whose behaviour changes with airspeed, phase-plane plots are not sufficient to determine their stability. To this purpose, bifurcation plots can be used, which can track the stability of a system over any range of airspeeds. Bifurcation plots can be constructed by obtaining the impulse response of a system at a given flight condition and then calculating the displacement of one of the degrees of freedom when the velocity of the same degree of freedom is zero. If the system is undergoing a LCO at a particular velocity, then the values of the displacement will be repeated. For example, in the case of Figure 9, the displacement takes two values at zero velocity. In Figure 10, there are six possible values of the displacement at zero velocity. In general, the number of points plotted on a bifurcation plot at a single flight condition is equal to twice the period index of a limit cycle, i.e. two points for a period-1 limit cycle, four points for a period-2 limit cycle, and so on. A bifurcation plot is obtained when all the values of the displacement when the velocity of that d.o.f. is zero are plotted for a range of discrete airspeeds.

It should be mentioned that, in many cases, the response of nonlinear systems depends upon initial conditions. This can happen when more than one stable singularities exist in the phase space, e.g. when two distinct stable limit cycles exist at the same airspeed. In that case, bifurcation diagrams are not unique but also depend on initial conditions. An experimental example of this behaviour can be found in Holden *et al.* (1995). However, all the systems examined in this work exhibit only one stable singularity in the phase space.

6. STABILITY OF THE AEROSERVOELASTIC SYSTEMS

The system equations were integrated in the time domain using Matlab and Simulink, employing a Runge–Kutta fourth- and fifth- order time-marching algorithm (Dormand & Prince 1980). The discontinuous nonlinearities were handled by pinpointing every occurrence of discontinuity to within machine accuracy. For example, for freeplay stiffness, every occurrence of $\beta = \pm\,\delta$ was solved for to within $\beta = \pm\,\delta \pm \varepsilon$, where ε is the machine accuracy.

TABLE 2
Stability of the aeroservoelastic systems

System	Stability regions					
Linear (m/s)	$<44{\cdot}9$	$>44{\cdot}9$				
No feedback	Stable	Flutter				
Linear (m/s)	$<53{\cdot}5$	$>53{\cdot}5$				
Feedback	Stable	Flutter				
Linear (m/s)	$<52{\cdot}1$	$>52{\cdot}1$				
Delayed feedback	Stable	Flutter				
Bilinear (m/s)	<37	37–44·6	$>44{\cdot}6$			
No feedback	Stable	LCO-1	Flutter			
Bilinear (m/s)	<51	51–53	53–53·3	$>53{\cdot}3$		
Feedback	Stable	LCO-1	LCO-2	Flutter		
Bilinear (m/s)	<48	48–50	50–51·1	51·5–51·8	$>51{\cdot}8$	
Delayed feedback	Stable	LCO-1	LCO-3	LCO-x	Flutter	
Freeplay (m/s)	<16	16–47·5	$>47{\cdot}5$			
No feedback	Stable	LCO-3	Flutter			
Freeplay (m/s)	<17	17–18	18–55	>55		
Feedback	Stable	LCO-1	LCO-3	Flutter		
Freeplay (m/s)	<17	17–18	18–51	51–52·3	$>52{\cdot}3$	
Delayed feedback	Stable	LCO-1	LCO-3	LCO-6	Flutter	
Backlash (m/s)	<8	8–13	13–34·5	34·5–36	36–44	>44
No feedback	Stable	LCO-x	LCO-1	LCO-2	LCO-1	Flutter
Backlash (m/s)	<8	8–53	>53			
Feedback	Stable	LCO-1	Flutter			
Backlash (m/s)	<8	8–48	48–51	51–52·1	$>52{\cdot}1$	
Delayed feedback	Stable	LCO-1	Period–doubling	LCO-1	Flutter	
Pitch limit (m/s)	$<45{\cdot}5$	45·5–57	>57			
	Stable	LCO-x	Flutter			
Friction (m/s)	<48	>48				
No feedback	Stable	Flutter				
Friction (m/s)	$<55{\cdot}2$	$>55{\cdot}2$				
Feedback	Stable	Flutter				
Friction (m/s)	$<53{\cdot}8$	$>53{\cdot}8$				
Delayed feedback	Stable	Flutter				

The impulse responses of the nonlinear systems described in Section 2 were calculated for a range of different airspeeds. The effect of including a control circuit was also investigated. Bifurcation plots were then generated in order to characterize the limit cycle behaviour. The key stability regions for each case are summarized in Table 2. In the table, LCO-n denotes a period-n LCO for $n = 1, 2, \ldots$, and LCO-x denotes a nonperiodic LCO.

6.1. STABILITY OF BILINEAR STIFFNESS SYSTEM

Aeroelastic systems with bilinear stiffnesses have already been extensively analysed in previous work, such as Yang & Zhao (1988). The system used here to provide a reference for the aeroservoelastic case differs from previous work in that it contains a bilinear stiffness element in the PCU. Hence, results are presented from the coupling of the bilinear system with the displacement feedback of Section 4.1. Figure 13 shows the bifurcation plot for the systems with bilinear pressure feedback spring. The plots are labelled "no feedback" for the uncontrolled system, "no delay" for the system with control feedback but no delay and "delay = dt" for the system with delayed control feedback. For airspeeds where the systems are stable (up to 45 m/s), only zeros are plotted.

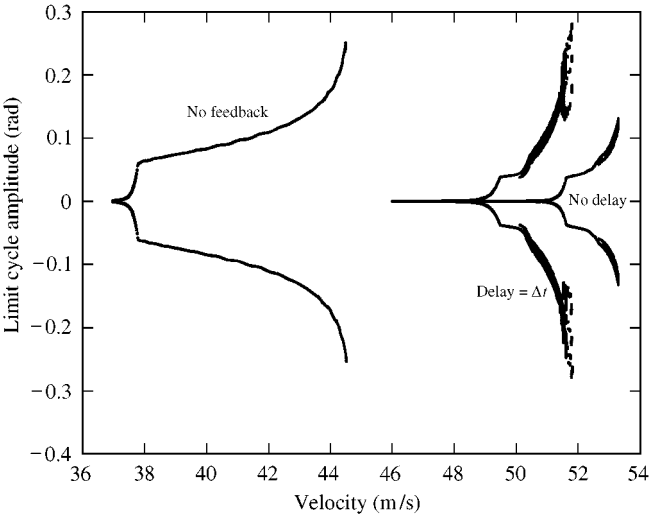

Figure 13. Bifurcation diagrams of system with bilinear spring.

Between 37 m/s and just over 44·6 m/s, the uncontrolled bilinear system undergoes LCOs. The limit cycles are period-1; hence, there are only two points plotted at each airspeed. The amplitudes of the limit cycles increase dramatically around 38 m/s. Between 38 and 42 m/s, the increase in LCO amplitude is slow. After 42 m/s, the amplitudes increase exponentially, which is a sign that the system is close to instability. At speeds above 44·6 m/s, the system becomes completely unstable and it flutters.

It has already been mentioned that the displacement feedback system was designed to stabilize the linear aeroservoelastic system. The two main considerations in this section are whether the feedback system can also stabilize the bilinear system and also what are the effects of delaying the feedback. It is of interest to note that the system with bilinear stiffness undergoes LCOs at airspeeds above the flutter speed of the linear system with stiffness K_1 and below the flutter speed of the linear system with stiffness K_2.

Figure 13 shows the bifurcation diagram for the bilinear system with feedback (not delayed). It can be seen that LCOs only begin to occur at airspeeds higher than 51 m/s. At 53 m/s, the LCOs switch from period-1 to period-2. Flutter occurs at 53·3 m/s which is only slightly lower than the flutter speed of the linear controlled system (see Table 2).

Consequently, the effect of the feedback is to stabilize the system, despite the bilinear actuator spring. Limit cycles appear later than in the open-loop system and they are of lower amplitude. Additionally, flutter is delayed by approximately 16%.

Delaying the feedback signal by one simulation time step has an adverse effect on the stability of the closed-loop system. Figure 13 also shows the bifurcation diagram for the bilinear system with delayed feedback. Limit cycles (period-1) first appear at 48 m/s but their amplitudes remain low up to an airspeed of just over 49 m/s. At 50 m/s, the limit cycles change to period-3. At 51·5 m/s, the system bifurcates to an even higher period. Finally, at 51·8 m/s, the system starts to flutter. Nevertheless, the system with delayed feedback is more stable than the open-loop system since limit cycles appear later and are initially of much smaller amplitude.

6.2. Stability of Freeplay System

As with bilinear stiffness, freeplay has been already thoroughly investigated, most recently in Kim & Lee (1996) and Conner *et al.* (1997), though not in a PCU. Here, the effect of

freeplay in conjunction with displacement feedback is of interest. Firstly, it should be mentioned that freeplay is a much more nonlinear function than bilinear stiffness and that its effects are more pronounced. With reference to the system investigated here, it should be noted that, since the stiffness is zero inside the freeplay region, the only source of stiffness in the control surface pitch direction is aerodynamic stiffness. This in turn signifies that LCOs are expected to be encountered at lower airspeeds than in the bilinear system.

The bifurcation diagram for the freeplay system with no feedback is shown in Figure 14. The system is stable up to an airspeed of 16 m/s when period-3 limit cycles occur. The amplitude of the LCO get larger in amplitude until flutter occurs at 47·5 m/s.

Figure 15 shows the bifurcation diagram for the freeplay system with undelayed feedback. The system is stable up to an airspeed of 17 m/s when period-1 limit cycles appear. At

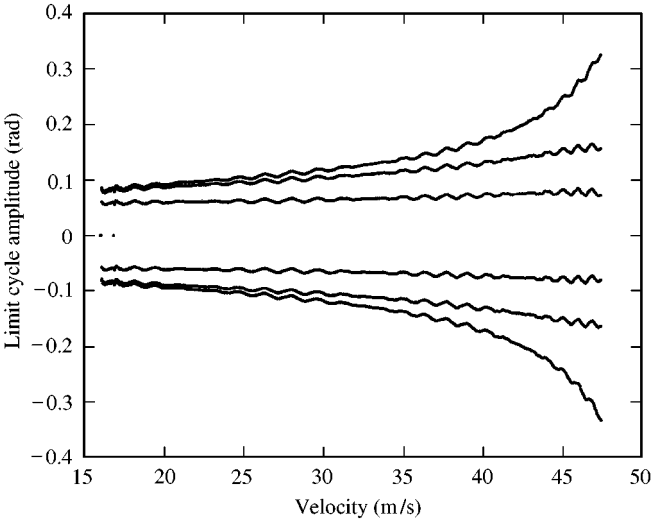

Figure 14. Bifurcation diagram of system with freeplay spring, no feedback.

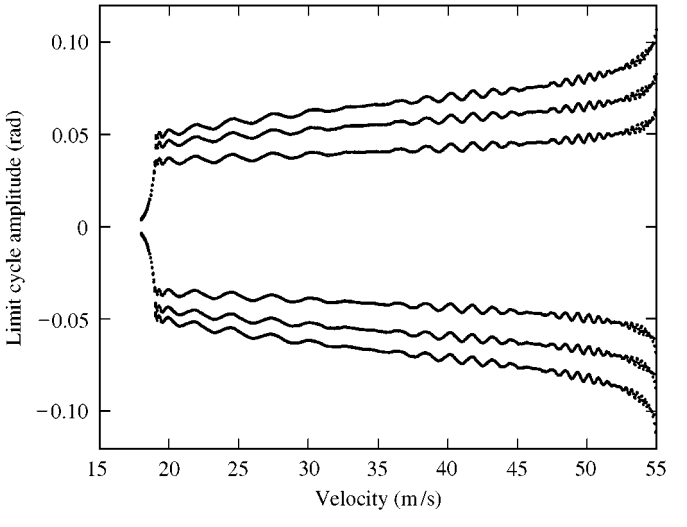

Figure 15. Bifurcation diagram of system with freeplay spring and feedback, no delay.

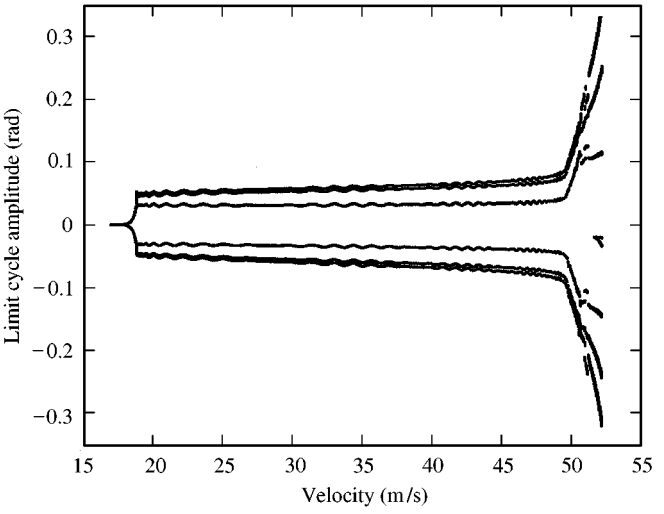

Figure 16. Bifurcation diagram of system with freeplay spring, feedback and delay.

18 m/s the limit cycles change to period-3. Finally, flutter occurs at 55 m/s. The feedback has stabilized the system by delaying the appearance of LCOs by 2 m/s and increasing the flutter speed by 16%. Additionally, the amplitudes of all limit cycles are lower than in the open-loop system.

Finally, Figure 16 shows the bifurcation diagram for the freeplay system with delayed feedback. Limit cycles first appear at 17 m/s and are period-2, as with the undelayed feedback. At 50 m/s, the amplitude of the limit cycles starts to drastically increase and at 51 m/s a bifurcation to period-6 limit cycles occurs. The system begins to flutter at 52·3 m/s.

Figure 16 shows that the main effects of this delay are to decrease the flutter airspeed and to increase the amplitude of high sub-critical LCOs. Nevertheless, as with the bilinear case, the delayed feedback system is more stable than the open-loop system since the flutter speed is increased by 10% and the limit cycles have smaller amplitudes than in the uncontrolled case.

6.3. Stability of System with Backlash

Figure 17 shows the bifurcation plot for the open and closed-loop systems with backlash in the pressure feedback spring. The open-loop system exhibits limit cycle behaviour from a very low airspeed (8 m/s). The limit cycles up to 13 m/s are very complex and nonperiodic. An example of such a limit cycle is shown in Figure 18 both in the phase-plane and in the time domain. Such behaviour generally occurs in the presence of a strong instability. In this case, it is caused by divergence at the low range of the flight envelope, where the aerodynamic stiffness is quite low. At airspeeds higher than 13 m/s, where the aerodynamic stiffness is sufficiently high, the LCOs are stabilized and become period-1. At 34·5 m/s, a bifurcation to period-2 limit cycles occurs but the system reverts back to period-1 LCOs at 36 m/s. Finally, flutter occurs at 44 m/s. Hence, the backlash introduces a very high level of instability, causing LCOs almost throughout the flight envelope.

Figure 17 also displays the bifurcation diagram for the system with backlash in the pressure feedback spring and undelayed feedback. Again, the first limit cycles appear at 8 m/s, but the displacement feedback does not allow divergence to occur, hence the LCOs

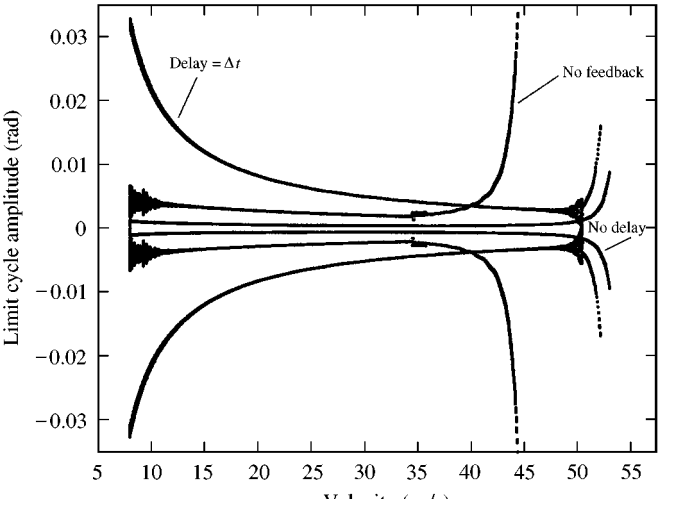

Figure 17. Bifurcation diagram of systems with backlash, open loop and closed loop.

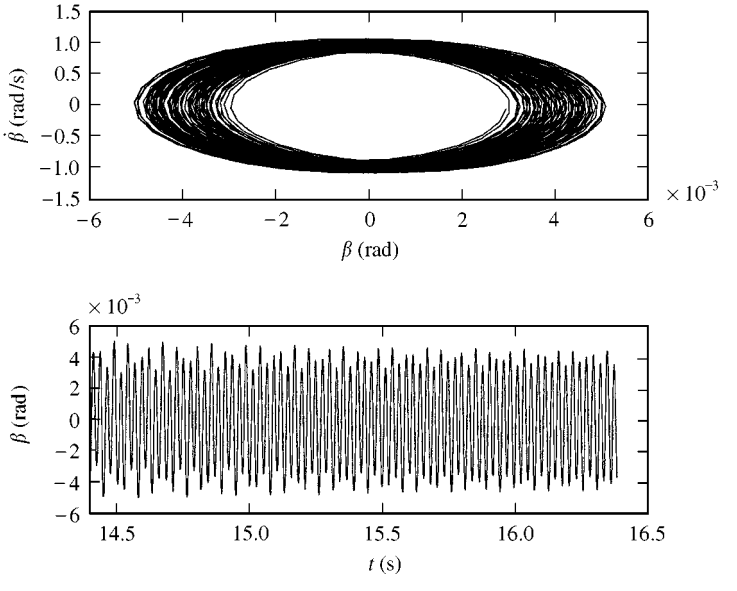

Figure 18. Example of aperiodic LCO from system with backlash and no feedback, $V = 9$ m/s.

are period-1. Flutter is delayed beyond the flutter airspeed of the open-loop system by high amplitude period-1 LCOs in the range 51–53 m/s. The controller has stabilized the system by decreasing the amplitude of the limit cycles, stabilizing the low-speed LCOs and increasing the flutter speed by 20%.

Finally, Figure 17 also shows the bifurcation diagram for the backlash system with delayed feedback. The low-speed LCOs are period-1 but have very high amplitude, even higher than those of the uncontrolled system, up until 40 m/s. At 48 m/s, the period index of the limit cycles starts to increase very fast. This behaviour is called period-doubling (Dimitriadis & Cooper 1999) and is, in general, an indication of impending instability. The LCOs revert back to period-1 at an airspeed of 51 m/s but flutter occurs shortly after that, at 52·1 m/s. In summary, the delayed feedback has increased the flutter speed of the

uncontrolled system by 18% but has increased the limit cycle amplitudes at the lower end of the speed-range.

6.4. Stability of System with Control Surface Pitch Limit

The feedback signal in the scheme described in Section 4.3 is zero unless the linear extrapolation of β, the control surface pitch degree of freedom, suggests that the value of β in the next step will be higher than the defined pitch limit, in which case the feedback signal is equal to $-a\beta$ where a is a gain coefficient. Consequently, it is obvious that, if the pitch limit were equal to zero, then the control law would be a linear proportional feedback. For the purposes of this work, the limit was set to $\pm 10^{\circ}$.

The effectiveness of the control scheme is demonstrated in Figure 19 where the control surface pitch is plotted against time. The dashed line is the demand signal fed to the control

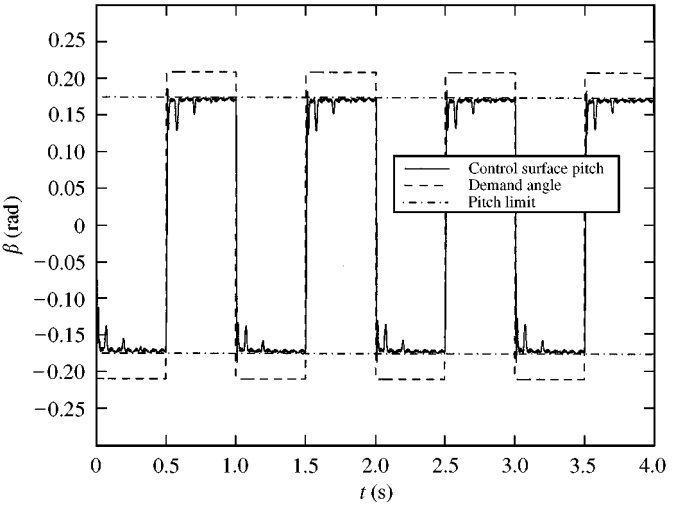

Figure 19. Performance of control surface pitch limiting control scheme.

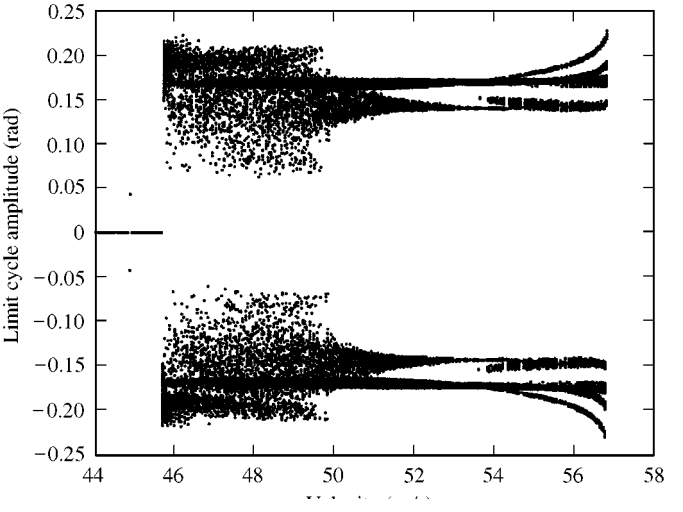

Figure 20. Bifurcation diagram of system with control surface pitch limit.

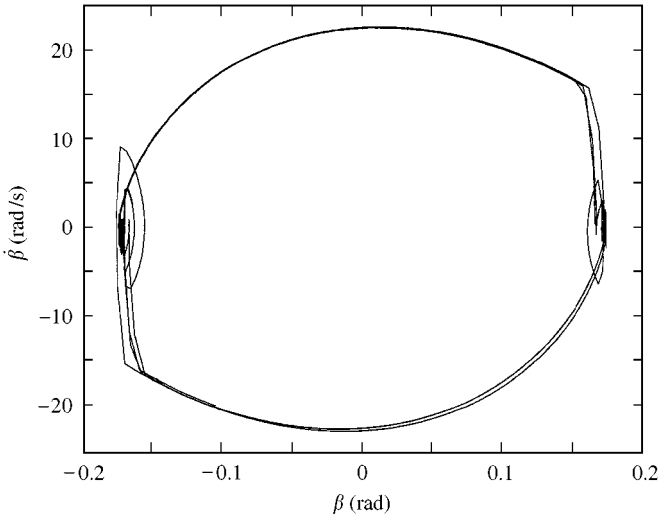

Figure 21. Limit cycle of system with control surface pitch limit at $V = 55$ m/s.

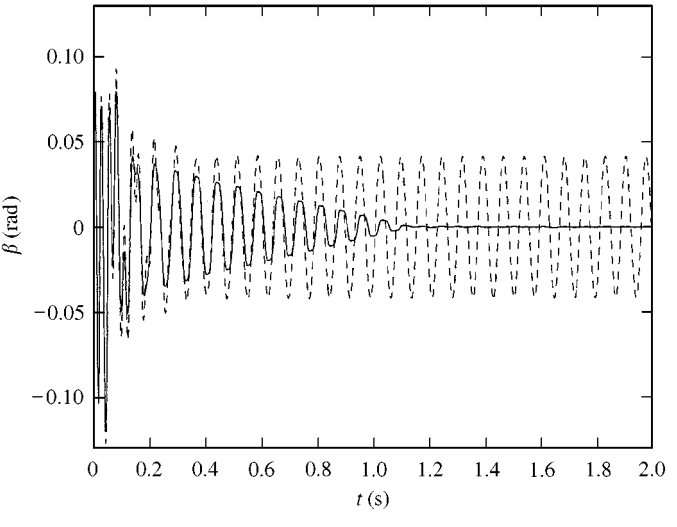

Figure 22. Comparison of responses of frictionless system and system with friction at $V = 44.9$ m/s: ——, $F_R = 0{\cdot}2$; – – –, $F_R = 0$.

surface through the power control unit. It can be seen that pitch rarely exceeds the limit of 10° (0.1745 rad), even though the demand angle is 12°. Since the control system only engages when the control surface pitch lies near the limit, it does not affect the decaying impulse response of the system. Hence, self-excited oscillations are only possible when the linear system flutters. In other words, the control system contains flutter by constraining the system response onto a limit cycle. This can be seen in Figure 20 where the bifurcation diagram for the pitch limited system is shown. Up to around 45·5 m/s the response is decaying. Limit cycles exist at airspeeds between 45·5 and 57 m/s. Beyond this range, the closed-loop system flutters. The flutter speed of the controlled system is 27% higher than that of the uncontrolled system. Figure 20 shows that the limit cycles are very complex since

many points appear at each airspeed, in fact so many that it is impossible to classify the limit cycles in terms of period. A phase-space plot of a limit cycle at an airspeed of 55 m/s is shown in Figure 21. The complicated shape of the limit cycles is due to the value of Δt in equation (4). In many cases, by the time the controller predicts an exceedence of the pitch limit, the exceedence has already happened. A lower value of Δt would give rise to better behaved limit cycles but might be less realistic.

6.5. Stability of System with Friction in the PCU

Friction is a mechanism that removes energy from the motion of a system. Given that the amplitude of the frictional force, F_R, is low enough not to cause stoppages, its main function is to effectively increase the damping present in the motion. A frictional force of varying amplitude was added to the open-loop linear, freeplay and bilinear systems. As was expected, the main consequence for all the systems was an increase in damping. This effect can be observed in Figure 22 where the control surface pitch impulse response of the open-loop, frictionless linear system is plotted on the same axes as that of the system with friction. The figure shows impulse responses at an airspeed very close to the flutter speed of the linear system. The response of the system with friction dies out after 1·1 s, while that of the frictionless system is completely undamped and remains at the same level forever.

Table 3
Increase of flutter speeds due to friction

System	Flutter speed, $F_R = 0{\cdot}0$ (m/s)	Flutter speed, $F_R = 0{\cdot}2$ (m/s)	% Increase
Linear	44·9	48	7%
Bilinear	44·6	46·8	5%
Freeplay	47·5	48·4	2%
Backlash	44	47·9	9%

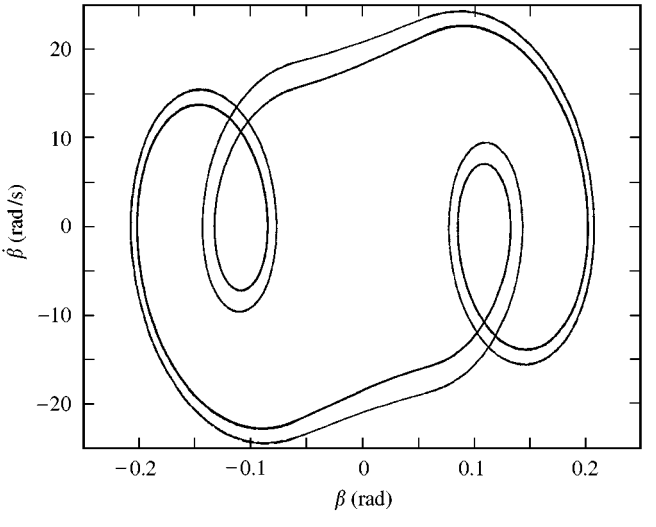

Figure 23. Comparison of limit cycles of freeplay system with and without friction at $V = 43$ m/s: ——, $F_R = 0{\cdot}2$; – – – (just visible), $F_R = 0$.

Friction does not cause limit cycles by itself, since it is an energy extraction mechanism. As such, it affected positively the stability of the systems investigated in this work. The flutter speeds of the linear, bilinear, freeplay and backlash systems were increased by the introduction of friction, even when F_R was low enough not to cause stoppages. Table 3 compares the the flutter speeds of all the open-loop systems with and without friction. The gains in flutter speed, for this particular value of frictional amplitude, are not as impressive as those achieved by the control systems. Additionally, the limit cycle amplitudes of the bilinear, freeplay and backlash systems were decreased, as indicated by Figure 23 which compares the limit cycles of the freeplay system with and without friction at an airspeed of 43 m/s

When F_R exceeds a certain level, stoppages in the motion occur and the stability of all the systems is affected dramatically. Figure 24 shows the variation of flutter airspeed for the

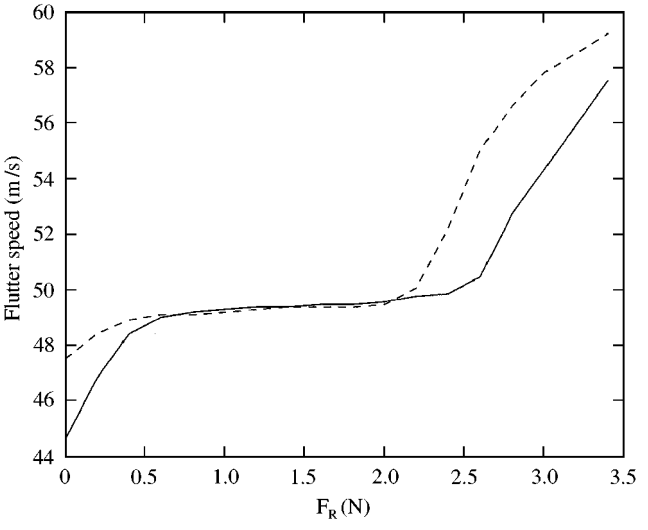

Figure 24. Variation of flutter speed of bilinear and freeplay systems with increasing frictional amplitude: ——, bilinear system with friction; – – –, freeplay system with friction.

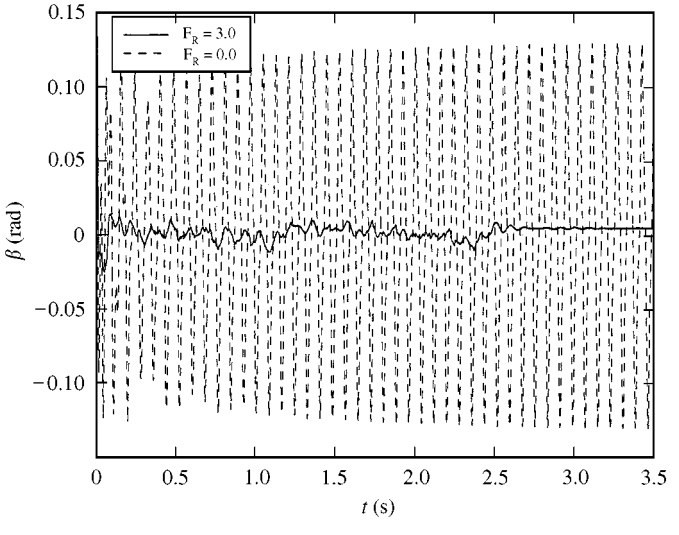

Figure 25. Comparison of responses of bilinear system with and without friction at $V = 50$ m/s.

freeplay and bilinear systems with friction of increasing amplitude. In both cases, the flutter speeds initially flatten towards a value of 49.5 m/s. However, at a particular value of the frictional amplitude (2 N for the freeplay system and 2.5 N for the bilinear system), the friction starts to cause stoppages and the LCOs that would have occurred in the absence of friction are inhibited. Additionally, the flutter speed is increased and keeps increasing at even higher values of F_R. The response of the bilinear system with friction of amplitude $F_R = 2$ N is compared to that of the frictionless bilinear system in Figure 25. It can be seen that, in the absence of friction, the system undergoes limit cycle oscillations. Friction suppresses the LCO by inhibiting the motion to such an extent that only irregular, low-amplitude oscillations are possible.

7. CONCLUSIONS

A simple bending-heave airfoil with control surface system has been used to explore the effect of nonlinearities on aeroservoelastic behaviour. It is possible for limit cycle oscillations to occur, which may be of high period and amplitude. The linear feedback that was applied still helped to stabilize the system, even in the presence of three types of nonlinearity. Delays in the feedback signals reduced the effectiveness of the control in all systems by a small amount. However, if the delay was too great, then instability occurred almost immediately. A nonlinear control law designed to limit the control surface pitch response was found to increase the flutter speed considerably by forcing the system to undergo limit cycle oscillations instead. Friction was found to improve the stability of the systems investigated here, when its amplitude took moderate values. At high values of the frictional amplitude, stoppages in the motion suppressed the system dynamics.

Throughout this work, it has been assumed that limit cycle behaviour is more stable than and, therefore, preferable to flutter. From a mathematical point of view this is corrects, however, from an engineering perspective, some of the LCOs that the aeroservoelastic systems underwent would be unacceptable. High-amplitude LCOs can negatively affect the structural rigidity and handling qualities of aeroservoelastic systems whilst, even lower amplitude LCOs can inrease the likelihood of fatigue failure. In order to determine which LCO amplitudes are preferable to flutter, for a particular aircraft, a much more detailed, case-specific analysis needs to be carried out. Additionally, more advanced aerodynamic modelling methods can be employed to investigate aeroservoelastic behaviour in the transonic flight regime.

REFERENCES

AGARD 1998 Numerical unsteady aerodynamic and aeroelastic simulation. AGARD Report 822.

BECKER, J. & VACCARO, V. 1995. Aeroservoelastic design, test verification and clearance of an advanced flight control system. *AGARD, Conference Proceedings CP*-566. Paper no. 22.

BREITBACH, E. 1978 Effects of structural nonlinearities on aircraft vibration and testing. AGARD, Report R-665.

CONNER, M. D., TANG, D. M., DOWELL, E. H. & VIRGIN, L. 1997 Nonlinear behaviour of a typical airfoil section with control surface freeplay: a numerical and experimental study. *Journal of Fluids and Structures* **11,** 89–109.

COOPER, J. E. & NOLL, T. T. 1995 Technical evaluation report on the 1995 specialists' meeting on advanced aeroservoelastic testing and data analysis. *AGARD, Conference Proceedings CP*-566. Paper T.

DIMITRIADIS, G. & COOPER, J. E. 1999 Limit cycle oscillation control and suppression. *Aeronautical Journal* **103,** 257–263.

DORMAND, J. R. & PRINCE, P. J. 1980 A family of embedded Runge–Kutta formulae. *Journal of Computational and Applied Mathematics* **6,** 19–26.

FRAMPTON, K. & CLARK, R. L. 1999 Experiments on control of limit cycle oscillations in a typical section. In *Proceedings of the 1999 AIAA/ASME/ASCE/AHS/ASC Structures, Structural Dynamics and Materials Conference*, St. Louis, MO, U.S.A.

HANCOCK, G. J., WRIGHT, J. R. & SIMPSON, A. 1985 On the teaching of the principles of wing flexure-torsion flutter. *Aeronautical Journal* **89,** 285–305.

HOLDEN, M., BRAZIER, R. E. J. & CAL, A. A. 1995 Effects of structural non-linearities on a tailplane flutter model. In *Proceeding of the CEAS International Forum on Aeroelasticity and Structural Dynamics*, Manchester, U.K. Paper no. 60.

KIM, S. H. & LEE, I. 1996 Aeroelastic analysis of a flexible airfoil with a freeplay non-linearity. *Journal of Sound and Vibration* **193,** 823–846.

LEE, I. & KIM, S. H. 1995 Aeroelastic analysis of a flexible control surface with structural nonlinearity. *Journal of Aircraft* **32,** 869–874.

LUBER, W. G. 1997 Flutter prediction on a combat aircraft involving backlash and actuator failures on control surfaces. In *Proceedings of the CEAS International Forum on Aeroelasticity and Structural Dynamics*, pp. 173–182, Rome, Italy.

MAHARAJ, D. Y., ROSENBORG, G. & COWLING, D. A. 1991 The modelling of actuator backlash in aeroservoelastic analysis and its effect on FCS/structural mode coupling. In *Proceedings of the International Forum on Aeroelasticity and Structural Dynamics*, pp. 394–403, Aachen, Germany.

MASTRODDI, F. & MORINO, L. 1996 Limit-cycle taming by nonlinear control with applications to flutter. *Aeronautical Journal* **100,** 389–396.

MORTON, S. A. & BERAN, P. S. 1999 Hopf bifurcation analysis of airfoil flutter at transonic speeds. *Journal of Aircraft* **36,** 421–429.

MUKHOPADHYAY, V. 1995 Flutter suppression control law design and testing for the Active Flexible Wing. *Journal of Aircraft* **32,** 45–51.

NOLL, T. 1993 Aeroservoelasticity. In *Flight Vehicle Materials, Structures and Dynamics-Assessment and Future Directions*, Chap. 3, pp. 179–212. New York: ASME.

PRICE, S. J., ALIGHANBARI, H. & LEE, B. H. K. 1995 The aeroelastic behaviour of a two-dimensional airfoil with bilinear and cubic structural nonlinearities. *Journal of Fluids and Structures* **9,** 175–193.

PRICE, S. J., LEE, B. H. K. & ALIGHANBARI, H. 1994 Postinstability behaviour of a two-dimensional airfoil with a structural nonlinearity. *Journal of Aircraft* **31,** 1395–1401.

VIPPERMAN, J. S., CLARK, R. L., CONNER, M. & DOWELL, E. H. 1998 Experimental active control of a typical section using a trailing edge flap. *Journal of Aircraft* **35,** 224–229.

WOOLSTON, D. S., RUNYAN, H. L. & BYRDSONG, T. A. 1955 Some effects of system nonlinearities in the problem of aircraft flutter. NACA Technical Note TN 3539.

WRIGHT, J. R. 1975 Flutter test analysis methods. Ph.D. thesis, University of Bristol, U.K.

YANG, Z. C. & ZHAO, L. C. 1988 Analysis of limit cycle flutter of an airfoil in incompressible flow. *Journal of Sound and Vibration* **123,** 1–13.

ZIMMERMANN, H. 1991 Aeroservoelasticity. *Computer Methods in Applied Mechanics and Engineering* **90,** 719–735.